

Basic Study

Development of a rat model of D-galactosamine/ lipopolysaccharide induced hepatorenal syndrome

Jing-Bo Wang, Hai-Tao Wang, Lu-Ping Li, Ying-Chun Yan, Wei Wang, Jing-Yang Liu, Yi-Tong Zhao, Wei-Shu Gao, Ming-Xiang Zhang

Jing-Bo Wang, Lu-Ping Li, Ying-Chun Yan, Wei Wang, Jing-Yang Liu, Yi-Tong Zhao, Wei-Shu Gao, Ming-Xiang Zhang, Cirrhosis Treatment Center, the Sixth People's Hospital of Shenyang, Shenyang 110006, Liaoning Province, China

Hai-Tao Wang, Department of General Surgery, the Affiliated Shenzhou Hospital of Shenyang Medical College, Shenyang 110001, Liaoning Province, China

Author contributions: Wang JB, Wang HT and Zhang MX contributed equally to this work, and all of them were involved in the design and performing of the experiment, data analysis and drafting of the article; Li LP, Yan YC and Gao WS participated in the design and performing of the study and biochemical test; Wang W, Liu JY and Zhao YT the completed hepatic and renal pathological examination, data analysis and drafting of the paper.

Institutional animal care and use committee statement: This study was approved by the Ethical Committee of Shenyang Sixth People's Hospital.

Conflict-of-interest statement: The authors declare no conflicts of interest.

Data sharing statement: No additional data are available.

Open-Access: This article is an open-access article which was selected by an in-house editor and fully peer-reviewed by external reviewers. It is distributed in accordance with the Creative Commons Attribution Non Commercial (CC BY-NC 4.0) license, which permits others to distribute, remix, adapt, build upon this work non-commercially, and license their derivative works on different terms, provided the original work is properly cited and the use is non-commercial. See: <http://creativecommons.org/licenses/by-nc/4.0/>

Correspondence to: Ming-Xiang Zhang, Professor, Cirrhosis Treatment Center, the Sixth People's Hospital of Shenyang, 85 Hepingnan Street, Heping District, Shenyang 110006, Liaoning Province, China. zhangmingxiang2014@126.com
Telephone: +86-24-23387410-116

Received: March 15, 2015

Peer-review started: March 15, 2015

First decision: April 13, 2015

Revised: June 3, 2015

Accepted: June 26, 2015

Article in press: June 26, 2015

Published online: September 14, 2015

Abstract

AIM: To develop a practical and reproducible rat model of hepatorenal syndrome for further study of the pathophysiology of human hepatorenal syndrome.

METHODS: Sprague-Dawley rats were intravenously injected with D-galactosamine and lipopolysaccharide (LPS) *via* the tail vein to induce fulminant hepatic failure to develop a model of hepatorenal syndrome. Liver and kidney function tests and plasma cytokine levels were measured after D-galactosamine/LPS administration, and hepatic and renal pathology was studied. Glomerular filtration rate was detected in conscious rats using micro-osmotic pump technology with fluorescein isothiocyanate-labelled inulin as a surrogate marker.

RESULTS: Serum levels of biochemical indicators including liver and kidney function indexes and cytokines all significantly changed, especially at 12 h after D-galactosamine/LPS administration [alanine aminotransferase, 3389.5 ± 499.5 IU/L; blood urea nitrogen, 13.9 ± 1.3 mmol/L; Cr, 78.1 ± 2.9 μ mol/L; K⁺, 6.1 ± 0.5 mmol/L; Na⁺, 130.9 ± 1.9 mmol/L; Cl⁻, 90.2 ± 1.9 mmol/L; tumor necrosis factor- α , 1699.6 ± 599.1 pg/mL; endothelin-1, 95.9 ± 25.9 pg/mL; $P < 0.05$ compared with normal saline control group]. Hepatocyte necrosis was aggravated gradually, which was most significant at 12 h after treatment with D-galactosamine/LPS, and was characterized by massive hepatocyte necrosis, while the structures of glomeruli,

proximal and distal tubules were normal. Glomerular filtration rate was significantly decreased to 30%-35% of the control group at 12 h after D-galactosamine/LPS administration [Glomerular filtration rate (GFR)₁, 0.79 ± 0.11 mL/min; GFR₂, 3.58 ± 0.49 mL/min·kgBW⁻¹; GFR₃, 0.39 ± 0.99 mL/min·gKW⁻¹]. The decreasing timing of GFR was consistent with that of the presence of hepatocyte necrosis and liver and kidney dysfunction.

CONCLUSION: The joint use of D-galactosamine and LPS can induce liver and kidney dysfunction and decline of glomerular filtration rate in rats which is a successful rat model of hepatorenal syndrome.

Key words: Hepatorenal syndrome; Animal model; Rat; D-galactosamine; Lipopolysaccharide

© The Author(s) 2015. Published by Baishideng Publishing Group Inc. All rights reserved.

Core tip: In this article, D-galactosamine was injected into SD rats *via* the caudal vein to establish a model of hepatorenal syndrome (HRS). Twelve hours after injection, serum level of tumor necrosis factor- α was significantly elevated while the glomerular filtration rate was significantly lowered. Hepatorenal function became obviously abnormal. Pathological findings showed massive necrosis of liver cells but normal kidney structure. Our animal model provided a good simulation of partial pathophysiological process of human HRS.

Wang JB, Wang HT, Li LP, Yan YC, Wang W, Liu JY, Zhao YT, Gao WS, Zhang MX. Development of a rat model of D-galactosamine/lipopolysaccharide induced hepatorenal syndrome. *World J Gastroenterol* 2015; 21(34): 9927-9935 Available from: URL: <http://www.wjgnet.com/1007-9327/full/v21/i34/9927.htm> DOI: <http://dx.doi.org/10.3748/wjg.v21.i34.9927>

INTRODUCTION

Hepatorenal syndrome (HRS) is a condition consisting of functional renal failure, progressive decline in glomerular filtration rate (GFR), sodium retention, azotemia and oliguria, and functional but not morphological kidney dysfunction, which often develops in patients with end-stage liver disease^[1-3]. Approximately 40%-80% of patients with end-stage liver disease, such as late fulminant hepatitis, advanced liver cirrhosis and liver malignant tumors, develop HRS in the presence of liver decompensation^[4,5]. Due to the lack of effective treatments^[6-9], the mortality rate of HRS is as high as 60%-80%^[10,11]. Therefore, there is an urgent need to develop a practical and reproducible animal model of HRS that can simulate the pathological process and biochemical changes of human HRS in order to explore the pathophysiology of HRS, provide

new targets for clinical prevention and treatment of HRS, and reduce its morbidity and mortality.

MATERIALS AND METHODS

Materials

Animals: One hundred and ninety male Sprague-Dawley (SD) rats of SPF grade, weighing 220 ± 20 g, were purchased from the Laboratory Animal Center of Academy of Military Medical Sciences Of Chinese PLA (certification number: SCXK-2007-0040). Before the start of experiments, the rats were reared in separated cages.

Drugs and reagents: D-galactosamine (D-GalN), lipopolysaccharide (LPS), and fluorescein isothiocyanate (FITC) labelled inulin (FITC-inulin) were purchased from Sigma. Alzet mini-osmotic pumps (model 2001) were purchased from Durect. Regenerated cellulose membrane dialysis tubing (MWCO1000) was purchased from Union Carbide Corporation. Rat tumor necrosis factor (TNF)- α and endothelin-1 (ET-1) detection kits were obtained from R&D.

Methods

Doses of D-GalN and LPS for animal modeling:

As previously described^[12-15], 30 male SD rats under ether anesthesia were intravenously injected with 400 mg/kg D-GalN and 32 μ g/kg LPS in normal saline *via* the tail vein. Twenty-one rats died within 24 h of drug delivery, and the survival rate at 24 h was 30%. Thus, 400 mg/kg and 32 μ g/kg were considered toxic doses of D-GalN and LPS for modeling, respectively.

Animal groups and treatments: One hundred and forty male SD rats were randomly divided into a normal saline control group (NS group), a D-GalN plus LPS group (G/L group), a D-GalN group (G group), and an LPS group (L group). Rats in the G/L group, G group and L group were anaesthetized with 0.8% pentobarbital sodium (40 mg/kg, intraperitoneal injection) 1, 3, 6, 9, 16, 12, and 24 h after drug delivery. The dead rats were excluded from the experiment. Except that 10 rats each at 12 and 16 h and 15 rats at 24 h were used in the G/L group, 5 rats were used at other time points in the G/L group and all time points in the other groups. Heart blood samples were taken for biochemical indicator and cytokine measurements. The abdominal cavity was opened, and a tissue sample measuring about 1.0 cm \times 0.8 cm \times 0.3 cm was taken from the right liver lobe and fixed in 10% formalin, and another tissue sample measuring 1 mm \times 1 mm \times 1 mm was taken from the renal cortex and fixed in 2.5% glutaraldehyde. The control group was intravenously injected with equal volume of normal saline *via* the tail vein.

Serum biochemical indicator and cytokine measurements: Blood samples were centrifuged, and

Table 1 Serum levels of biochemical indicators and cytokines in rats of each group (mean \pm SE)

Group	ALT (IU/L)	BUN (mmol/L)	Cr (μ mol/L)	K ⁺ (mmol/L)	Cl ⁻ (mmol/L)	Na ⁺ (mmol/L)	TNF- α (pg/mL)	ET-1 (pg/mL)
NS (n = 5)	37.1 \pm 1.4	5.2 \pm 0.7	71.3 \pm 1.9	5.0 \pm 0.5	103.4 \pm 1.0	140.9 \pm 1.5	67.5 \pm 8.9	15.9 \pm 2.1
G/L-1 h (n = 5)	49.1 \pm 2.4 ^c	9.3 \pm 1.8 ^{a,c}	69.9 \pm 2.6 ^c	6.1 \pm 0.7 ^a	108.1 \pm 2.1 ^{a,c}	146.0 \pm 1.8 ^{a,c}	300.9 \pm 78.5	9.9 \pm 1.8
G/L-3 h (n = 5)	97.0 \pm 19.7 ^c	9.9 \pm 0.4 ^{a,c}	59.8 \pm 1.7 ^c	6.9 \pm 0.6 ^a	105.5 \pm 1.5 ^{a,c}	147.4 \pm 1.9 ^{a,c}	219.3 \pm 100.1	12.5 \pm 2.9
G/L-6 h (n = 5)	602.1 \pm 188.7 ^c	10.5 \pm 0.7 ^{a,c}	74.1 \pm 1.6 ^a	5.9 \pm 0.6	103.2 \pm 2.0 ^c	145.9 \pm 0.9 ^c	200.1 \pm 56.2	28.9 \pm 7.1
G/L-9 h (n = 5)	1858.1 \pm 700.9 ^{a,c}	10.0 \pm 0.6 ^{a,c}	70.1 \pm 1.3 ^{a,c}	5.7 \pm 0.5	99.8 \pm 1.4 ^c	140.5 \pm 1.1 ^c	611.6 \pm 186.9	50.1 \pm 20.1
G/L-12 h (n = 10)	3389.5 \pm 499.5 ^a	13.9 \pm 1.3 ^a	78.1 \pm 2.9 ^a	6.1 \pm 0.5 ^a	90.2 \pm 1.9 ^a	130.9 \pm 1.9 ^a	1699.1 \pm 599.1 ^a	95.9 \pm 25.9 ^a
G/L-16 h (n = 10)	3895.5 \pm 300.1 ^a	12.3 \pm 0.9 ^a	69.1 \pm 3.0 ^a	5.4 \pm 0.4	89.9 \pm 1.3 ^a	141.5 \pm 1.1 ^{a,c}	765.3 \pm 398.5	73.9 \pm 20.6 ^a
G/L-24 h (n = 15)	3223.6 \pm 466.1 ^a	8.8 \pm 0.6 ^{a,c}	70.9 \pm 1.9 ^a	5.8 \pm 0.7	98.3 \pm 1.5 ^{a,c}	142.0 \pm 1.6 ^c	309.1 \pm 92.9	30.9 \pm 8.1
G-12 h (n = 5)	87.9 \pm 15.9 ^c	7.9 \pm 0.6 ^{a,c}	57.4 \pm 1.8 ^c	5.2 \pm 0.5 ^c	97.9 \pm 1.4 ^c	142.1 \pm 1.5 ^c	78.3 \pm 21.0 ^c	21.5 \pm 5.1 ^c
L-12 h (n = 5)	48.1 \pm 6.3 ^c	8.1 \pm 0.5 ^{a,c}	60.7 \pm 1.0 ^{a,c}	5.5 \pm 0.4 ^{a,c}	97.9 \pm 1.9 ^{a,c}	140.9 \pm 1.8 ^c	48.9 \pm 14.0 ^c	21.9 \pm 3.9 ^c

^a*P* < 0.05 vs NS; ^c*P* < 0.05 vs GalN/LPS 12 h. D-GalN: D-galactosamine; LPS: Lipopolysaccharide; TNF- α : Tumor necrosis factor α ; ET-1: Endothelin-1; G: D-GalN; L: LPS; ALT: Alanine aminotransferase; BUN: Blood urea nitrogen.

500 μ L of supernatants were used for liver and kidney function detection. The remaining serum samples were aliquoted and stored at -80 $^{\circ}$ C for measurement of TNF- α and ET-1 using commercial ELISA kits according to the manufacturer's instructions.

Liver and kidney histopathology: Liver tissue was paraffin embedded, fixed and cut into sections (4.0 μ m). After conventional HE staining, the sections were observed under a light microscope to evaluate liver cell necrosis. Electron microscope samples were routinely dehydrated, embedded, and prepared as semi-thin sections. Following toluidine blue staining, the sections were positioned under a light microscope. After double staining with uranium acetate and lead citrate, renal tissue ultrastructure was observed using a JEOL JEM-1230 transmission electron microscope and photographed.

GFR determination: Microosmotic pump implantation was performed as previously described^[16,17]. In brief, 24% FITC-inulin solution was dialyzed in 1000 mL normal saline at room temperature for 24 h to make the concentration decline to 8%. After sterilization using a 0.22 μ m syringe driven filter, the solution was injected into microosmotic pumps according to the manufacturer's instructions, and the pumps were soaked in normal saline for 4-6 h. The rats were anesthetized with sodium pentobarbital, and a 0.5 cm incision was made along the ventral midline under the rib nest. Two microosmotic pumps with FITC-inulin solution were implanted in the left and right sides of the abdominal cavity, respectively. After suturing the incision, the rats were reared in separated cages, and the status of the rats was observed and body weight measured daily.

For serum FITC-inulin determination, rats were divided into an NS group, a G/L-12 h group, a G-12 h group, and an L-12 h group. Seven days after pump implantation, the animals were modeled as described above. Blood samples were collected 12 h later and centrifuged. For each 400 μ L of supernatant, 100 μ L of 0.5 mol/L HEPES buffer (pH 7.4) was added. The FITC

fluorescence of the mixture was determined using a fluorescence spectrophotometer, with excitation wavelength set at 485 nm and emission wavelength at 538 nm.

GFR was measured as previously described^[16,18]. The equation $GFR = R/[Iss]$ (where R is the pumping velocity of FITC-inulin and [Iss] is the constant FITC-inulin concentration in blood) was used to calculate GFR for rats of all groups. The units of measurements were as follows: GFR_1 (mL \cdot min⁻¹); GFR_2 (mL \cdot min⁻¹ \cdot kgBW⁻¹) = GFR_1/BW [where BW is the body weight (kg) of rats]; GFR_3 (mL \cdot min⁻¹ \cdot gKW⁻¹) = GFR_1/KW [where KW is the weight (g) of the two kidneys of rats].

Statistical analysis

SPSS 13.0 software was used for all statistical analyses. Numerical data are expressed as the mean \pm SE. Means following a normal distribution and having homogeneity of variance were compared using one-way analysis of variance among groups, otherwise the rank-sum test was used. *P*-values < 0.05 were considered statistically significant.

RESULTS

General status and survival rate

Rats in the G/L group exhibited reduced food ingestion, drinking and activity 6-8 h after drug delivery, slow movements and reduced response to stimuli at 12 h, and shortness of breath, disappearance of the ability to resist capture, and slight limb tremors at 13-19 h. The survival rate at 24 h for rats in the G/L group was 30%, and the mean survival duration was 18.2 \pm 3.7 h.

Serum levels of biochemical indicators and cytokines

As shown in Table 1, alanine aminotransferase (ALT) levels in the G/L group began to rise at 1 h after treatment, significantly rose at 12 h, peaked at 16 h (*P* = 0.000 vs NS), and began to fall at 24 h. blood urea nitrogen and Cr levels in the G/L group began to rise at 1 h and peaked at 12 h (*P* = 0.000 vs NS). K⁺, Na⁺ and Cl⁻ concentrations in the G/L group showed

obvious abnormalities at 12 h. Serum TNF- α and ET-1 levels peaked at 12 h in the G/L group ($P = 0.003$, 0.000 vs NS).

Gross morphological changes in the liver

Grossly, the liver of rats in the NS control group had a normal morphology. The surface of the liver was fine granular, the liver had a ruddy color, and the texture was slightly tough. For rats in the G/L group, scattered bleeding spots were visible on the liver surface at 6 h; the liver was congested, showed a deep red color and had more bleeding spots at 9 h; at 16, 12, and 24 h, the liver showed a deep purple color, and had significant congestion, swelling, and diffused bleeding spots, and the section plane of the liver showed dark red congestion or overflow of yellow chylous necrotic fluid.

Histopathological changes of the liver and kidney

For rats in the NS group, hepatocytes were arranged in chords under a light microscope, cell nuclei were clearly visible, cell membrane was intact, and the portal area and central veins were normal. For the G/L group, hepatocytes around the central veins showed focal necrosis and cell nuclei disappeared at 6 h; focal hepatocyte necrosis around the central veins became more significant and was fused together, and cell nuclei dissolved and disappeared at 9 h; at 12 h, hepatocytes showed massive necrosis, cords disappeared, fibrous septa collapsed, and there were no degenerated hepatocytes but there was massive red blood cell infiltration; at 16 and 24 h, massive hemorrhagic hepatic necrosis was visible (Figures 1 and 2).

Glomerular basement membrane was intact, and the pedicles of podocytes could be clearly seen. The base of cuboidal epithelial cells of the proximal and distal tubules showed plasma membrane infolds, in which mitochondria with intact cristae were visible. The microvilli on the luminal surface of proximal tubules were long and thick, while those on the luminal surface of distal tubules were short and sparse (Figure 3).

GFR for rats in the NS, G/L-12 h, G-12 h and L-12 h groups

GFR₁, GFR₂ and GFR₃ in the G/L group decreased most significantly compared with the NS group ($P < 0.05$), suggesting that GFR decreased significantly in HRS. GFR in the G/L group also differed significantly from those in the G and L groups ($P < 0.05$), which excluded the possible effect of D-GalN and LPS on GFR (Figure 4A-C).

DISCUSSION

The pathogenesis of HRS associated with fulminant hepatic failure (FHF) is complex and remains unclear^[19]. Because of the lack of effective treatments, the mortality of HRS is high. Therefore, understanding

the mechanisms of development and progression of HRS and use of multi-targeted combination treatment are of great importance for reducing the morbidity and mortality of HRS. The development of an animal model with good stability and reproducibility is the basis for these studies, and for this reason, we sought to develop a rat model of HRS in this study.

LPS is a toxic component of the Gram-negative (G⁻) bacterial cell wall, and D-GalN^[20,21] can increase the sensitivity of liver cells to LPS^[8,9] and induce liver cell apoptosis. Therefore, in the presence of low dose LPS, D-GalN can cause liver cell necrosis and result in FHF^[22-24] as well as abnormally elevated serum TNF- α . TNF- α is therefore considered to be a trigger of the cascade of inflammatory mediators and be closely related to the pathophysiology of FHF^[25-27]. In the present study, after rats were treated with D-GalN plus LPS, liver and kidney damage was most significant at 12 h after treatment and ALT was as high as 3000-4000 IU/L. Renal damage was parallel to the liver damage. Of note, potassium concentration showed an obvious rise at 3 h after treatment, which may be due to the renal tubular ion exchange dysfunction in early renal damage.

HRS is characterized by a progressive decline in GFR^[28]. Therefore, GFR is an important index for judging whether an HRS model is developed successfully or not. Clearance of inulin is the gold standard for GFR estimation, and labelling of inulin with FITC allows for detection of trace amounts of inulin and significantly improves the detection sensitivity. In previous studies, FITC-inulin has been used successfully to determine GFR in rats under anesthesia^[29,30]. There are two main types of GFR detection: (1) determination of urinary excretion rate of inulin^[31]; and (2) determination of inulin clearance rate based on plasma clearance kinetics^[32,33]. The present study adopted the urinary excretion rate method (without need of urine collection) to determine GFR as previously described by Qi *et al.*^[16] This method requires the implantation of two microosmotic pumps (Alzet microosmotic pump is an one-time sterile pump with a volume of $200 \pm 8 \mu\text{L}$, a pumping velocity of $1 \mu\text{L/h}$, and a service life of 7 d) in the abdominal cavity of rats, and they can continuously to pump FITC-inulin solution into the abdominal cavity, where it can enter into the bloodstream *via* peritoneal absorption. On day 7 after pump implantation when blood concentrations of inulin were stable, FITC fluorescence was measured to calculate GFR using the formula $\text{GFR} = R/\text{GFR}(\text{Iss})$ to ensure the accuracy of results.

GFR reported in previous studies varied greatly, and the present study calculated three different forms of GFR, to exclude the possible influence of body weight and kidney weight on GFR. GFR is a kinetic parameter that changes along with the change of physiological factors. The GFR for rats in the waking state was only 60% of the GFR for the same group of rats

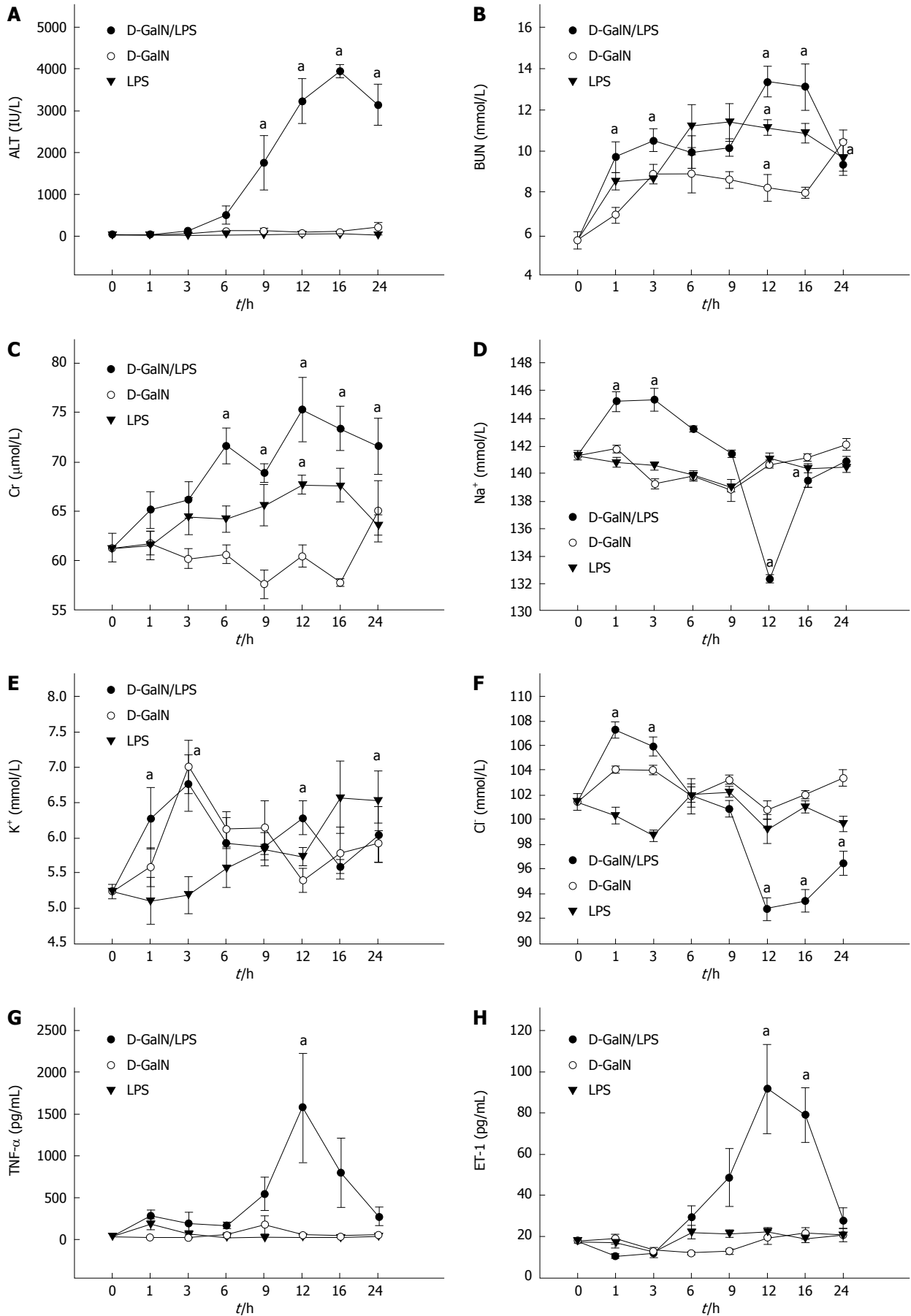


Figure 1 Serum levels of biochemical indicators and cytokines. D-GalN 400 mg/kg and LPS 32 μ g/kg in normal saline were intravenously injected via the tail vein. A: ALT (IU/L); B: BUN (mmol/L); C: Cr (μ mol/L); D: Na⁺ (mmol/L); E: K⁺ (mmol/L); F: Cl⁻ (mmol/L); G: TNF- α (pg/mL); H: ET-1 (pg/mL). * P < 0.05, G/L vs NS. D-GalN: D-galactosamine; LPS: Lipopolysaccharide; TNF- α : Tumor necrosis factor α ; ET-1: Endothelin-1; ALT: Alanine aminotransferase; BUN: Blood urea nitrogen.

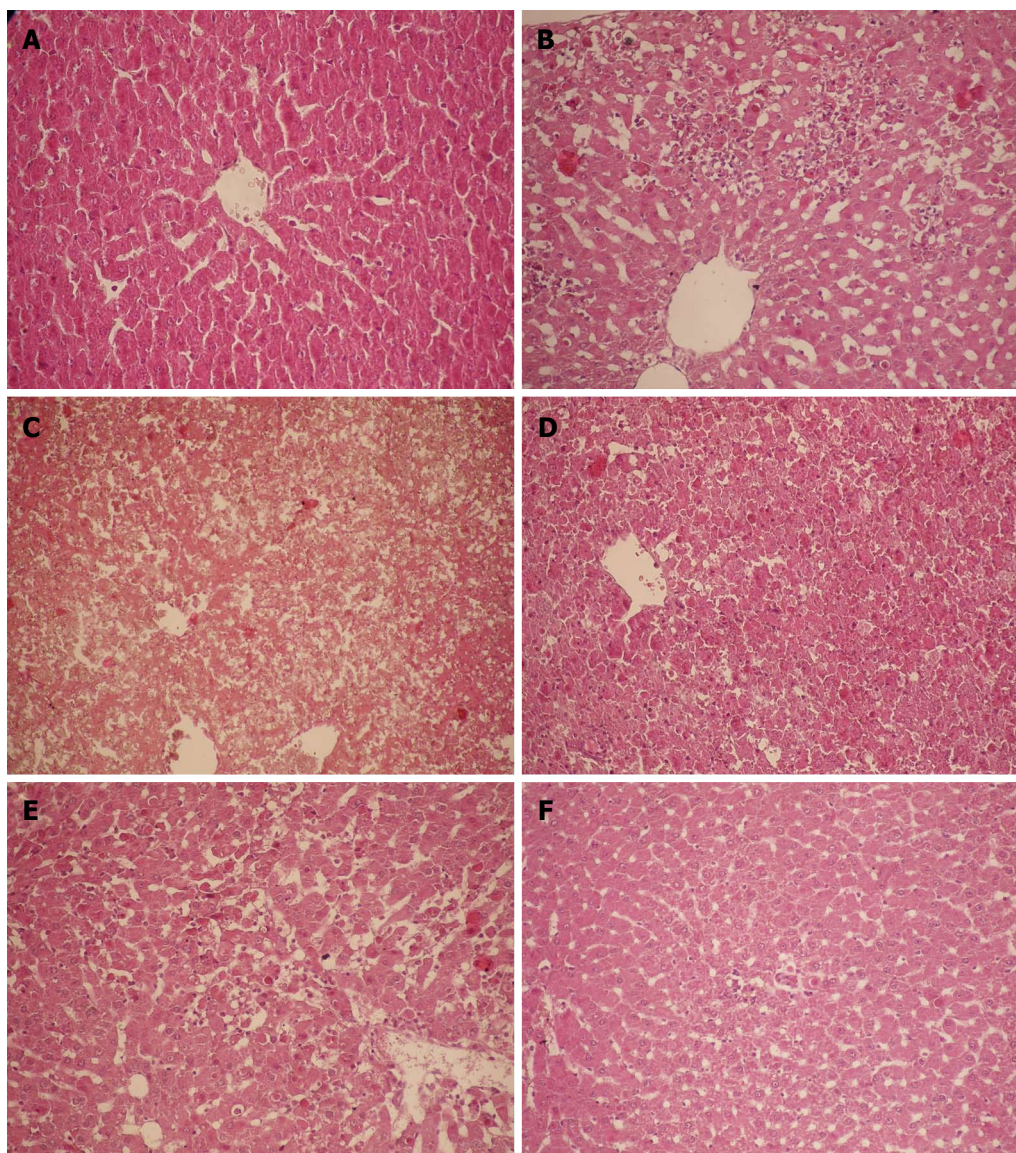


Figure 2 Histopathology of the liver (HE, × 200). A: In the NS group, hepatocytes were arranged in cords; B: In the GalN/LPS group at 6 h, focal necrosis of hepatocytes was visible; C: In the GalN/LPS group at 12 h, massive hemorrhagic hepatic necrosis was visible; D: In the GalN/LPS group at 24 h, massive hemorrhagic hepatic necrosis was visible; E: In the GalN group at 12 h, focal necrosis of hepatocytes was visible; F: In the LPS group at 12 h, hepatocytes began to show necrosis, and incomplete necrosis was observed in some hepatocytes. D-GalN: D-galactosamine; LPS: Lipopolysaccharide; NS: Normalsaline.

under anesthesia^[34]. The present study determined GFR in rats in the waking state to exclude the effect of anesthesia. The results showed that GFR in the necrosis group dropped to 33.4% of that in the normal control group, suggesting that glomerular filtration function is decreased obviously in HRS.

To rule out the influence of D-GalN and LPS on liver and kidney function, we also ran a D-GalN group and an LPS group as controls in addition to the normal saline control group. We found that hepatocyte necrosis progressed rapidly, and massive hemorrhagic hepatic necrosis appeared at 12 h, which is similar to pathological changes in human FHF, and the timing of these changes is consistent with that of the presence of liver and kidney dysfunction and GFR decline. In contrast, the structures of glomeruli, proximal and distal tubules for rats of all groups were normal, in line

with the characteristics of HRS, in which the kidneys have only functional changes, but not morphological changes.

TNF- α participates in a variety of pathophysiological processes in humans and animals, and is the main factor to cause severe liver disease. When HRS occurs, blood TNF- α level is abnormally increased, which is associated with urea nitrogen and creatinine levels. Treatment with pentoxifylline (a synthetic TNF- α inhibitor) can improve renal function and reduce the occurrence of HRS^[35,36]. ET-1 is a potent vasoactive peptide, which can adjust the GFR and affect kidney function by inducing the contraction of glomerular mesangial cells and renal afferent arterial smooth muscle cells. This study demonstrated that serum TNF- α and ET-1 levels increased significantly in rats with HRS, and the timing is consistent with that of

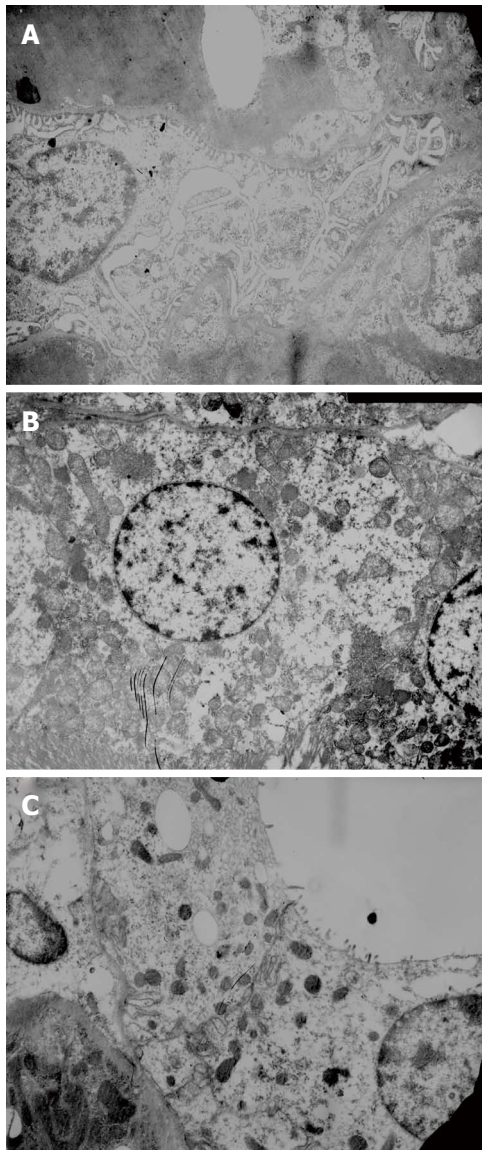


Figure 3 Histopathology of the kidney. A: Glomeruli: Glomerular basement membrane was intact, and the pedicles of podocytes and fenestrations on endothelial cells could be clearly seen; B: Proximal tubules: The base of cuboidal epithelial cells of proximal tubules showed many plasma membrane infolds, in which many mitochondria with intact cristae were visible, and the microvilli on the luminal surface of proximal tubules were long and thick; C: Distal tubules: The base of cuboidal epithelial cells of distal tubules also contained plasma membrane infolds, in which many mitochondria were visible. The microvilli on the luminal surface of distal tubules were short and sparse.

the presence of liver and kidney dysfunction and liver pathological changes, suggesting that $\text{TNF-}\alpha$ and ET-1 play an important role in the pathogenesis of HRS.

In conclusion, the joint use of D-GalN and LPS can successfully induce HRS in male SD rats. This model is stable and easy to reproduce, and the induced HRS has similar pathophysiology to human HRS and can be used to study the pathogenesis of HRS and screen drugs. The present study partially simulates the pathophysiological process of human HRS in rats.

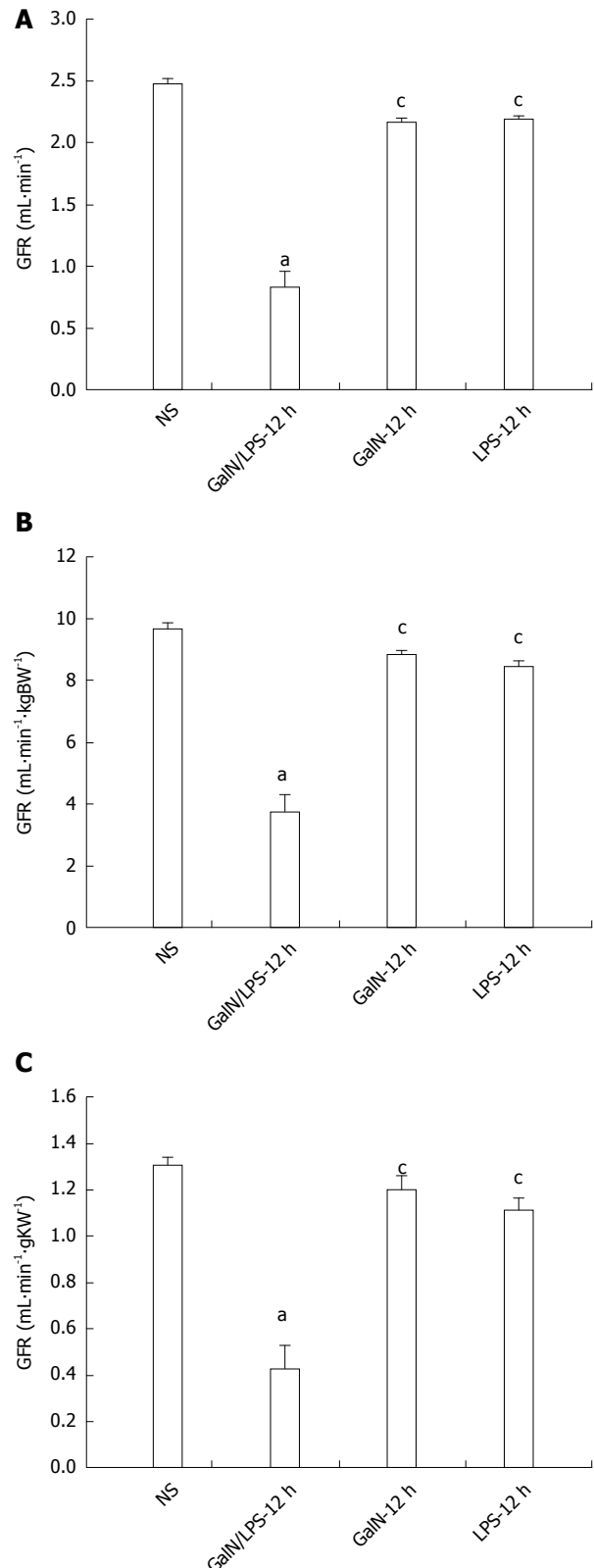


Figure 4 Comparisons of glomerular filtration rate for rats in each group. A: GFR_1 ($\text{mL}\cdot\text{min}^{-1}$); B: GFR_2 ($\text{mL}\cdot\text{min}^{-1}\cdot\text{kgBW}^{-1}$); C: GFR_3 ($\text{mL}\cdot\text{min}^{-1}\cdot\text{gKW}^{-1}$). GFR_1 , GFR_2 and GFR_3 decreased significantly in the GalN/LPS group compared with the NS, GalN and LPS groups (^a $P < 0.05$ vs NS; ^c $P < 0.05$ vs GalN/LPS-12 h). D-GalN: D-galactosamine; LPS: Lipopolysaccharide; GFR: Glomerular filtration rate; NS: Normalsaline.

COMMENTS

Background

Hepatorenal syndrome (HRS), usually occurs in patients with end-stage liver disease, is a condition consisting of functional renal failure, progressive decline in glomerular filtration rate (GFR), sodium retention, azotemia and oliguria, and functional but not morphological kidney dysfunction. In the presence of liver decompensation, HRS may occur in about 40%-80% of patients. Due to lack of effective therapeutics, the mortality rate of HRS patients may reach 60%-80%. Therefore, an animal model of HRS is urgently needed to investigate the pathogenic mechanism of human HRS, which will provide new targets for clinical treatment.

Research frontiers

Currently, the mechanism of HRS remains unclear. Some studies considered that tumor necrosis factor- α is the initiation factor of HRS. It causes high expression of type I IP α R, renal vascular contraction, and decreases in GFR by TNFR α /PC-PLC/PKC α signal transduction pathway. There are relevantly few studies focusing on establishment of animal models and determination of GFR by abdominal implantation of miniosmotic pumps is internationally advanced.

Innovations and breakthroughs

Determination of GFR by abdominal implantation of miniosmotic pumps is the main innovative point in this article. In comparison with previous methods, this technique was simple and operable, and there was no need to collect 24-h urine samples. Meanwhile, the determination was performed without anaesthesia, which avoided influences on the renal blood flow and GFR. Therefore, the result was very close to that under normal conditions.

Applications

Further studies on the mechanisms of HRS using our animal model may provide new targets for clinical treatments, so as to achieve early diagnosis and multiple target inventions for HRS and decrease the morbidity and mortality rates.

Peer-review

This is a very good study about D-galactosamine/lipopolysaccharide (LPS) induced hepatorenal syndrome. The study is well designed. In this study, the authors developed a practical and reproducible rat model of hepatorenal syndrome for further study of the pathophysiology of human hepatorenal syndrome. Rat models were intravenously injected with D-galactosamine and LPS to induce fulminant hepatic failure, and develop a model of hepatorenal syndrome. The results are interesting.

REFERENCES

- Schrier RW, Shchekochikhin D, Ginès P. Renal failure in cirrhosis: prerenal azotemia, hepatorenal syndrome and acute tubular necrosis. *Nephrol Dial Transplant* 2012; **27**: 2625-2628 [PMID: 22492830 DOI: 10.1093/ndt/gfs067]
- European Association for the Study of the Liver. EASL clinical practice guidelines on the management of ascites, spontaneous bacterial peritonitis, and hepatorenal syndrome in cirrhosis. *J Hepatol* 2010; **53**: 397-417 [PMID: 20633946 DOI: 10.1016/j.jhep.2010.05.004]
- Martín-Llahí M, Guevara M, Torre A, Fagundes C, Restuccia T, Gilabert R, Solà E, Pereira G, Marinelli M, Pavesi M, Fernández J, Rodés J, Arroyo V, Ginès P. Prognostic importance of the cause of renal failure in patients with cirrhosis. *Gastroenterology* 2011; **140**: 488-496.e4 [PMID: 20682324 DOI: 10.1053/j.gastro.2010.07.043]
- Montoliu S, Ballesté B, Planas R, Alvarez MA, Rivera M, Miquel M, Masnou H, Cirera I, Morillas RM, Coll S, Sala M, García-Retortillo M, Cañete N, Solà R. Incidence and prognosis of different types of functional renal failure in cirrhotic patients with ascites. *Clin Gastroenterol Hepatol* 2010; **8**: 616-22; quiz e80 [PMID: 20399905 DOI: 10.1016/j.cgh.2010.03.029]
- Fagundes C, Ginès P. Hepatorenal syndrome: a severe, but treatable, cause of kidney failure in cirrhosis. *Am J Kidney Dis* 2012; **59**: 874-885 [PMID: 22480795 DOI: 10.1053/j.ajkd.2011.12.032]
- Angeli P, Morando F. Optimal management of hepatorenal syndrome in patients with cirrhosis. *Hepat Med* 2010; **2**: 87-98 [PMID: 24367209 DOI: 10.2147/HMER.S6918]
- Rössle M, Gerbes AL. TIPS for the treatment of refractory ascites, hepatorenal syndrome and hepatic hydrothorax: a critical update. *Gut* 2010; **59**: 988-1000 [PMID: 20581246 DOI: 10.1136/gut.2009.193227]
- Caraceni P, Santi L, Mirici F, Montanari G, Bevilacqua V, Pinna AD, Bernardi M. Long-term treatment of hepatorenal syndrome as a bridge to liver transplantation. *Dig Liver Dis* 2011; **43**: 242-245 [PMID: 20833118 DOI: 10.1016/j.dld.2010.08.001]
- Gonwa TA, Wadei HM. The challenges of providing renal replacement therapy in decompensated liver cirrhosis. *Blood Purif* 2012; **33**: 144-148 [PMID: 22269395 DOI: 10.1159/000334149]
- Nadim MK, Kellum JA, Davenport A, Wong F, Davis C, Pannu N, Tolwani A, Bellomo R, Genyk YS. Hepatorenal syndrome: the 8th International Consensus Conference of the Acute Dialysis Quality Initiative (ADQI) Group. *Crit Care* 2012; **16**: R23 [PMID: 22322077 DOI: 10.1186/cc11188]
- Lee JP, Kwon HY, Park JI, Yi NJ, Suh KS, Lee HW, Kim M, Oh YK, Lim CS, Kim YS. Clinical outcomes of patients with hepatorenal syndrome after living donor liver transplantation. *Liver Transpl* 2012; **18**: 1237-1244 [PMID: 22714872 DOI: 10.1002/lt.23493]
- Saracyn M, Wesołowski P, Nowak Z, Patera J, Kozłowski W, Wańkowicz Z. [Role of nitric oxide system in pathogenesis of experimental model of hepatorenal syndrome]. *Pol Merkur Lekarski* 2008; **24**: 293-297 [PMID: 18634358]
- Hijikawa T, Kaibori M, Uchida Y, Yamada M, Matsui K, Ozaki T, Kamiyama Y, Nishizawa M, Okumura T. Insulin-like growth factor 1 prevents liver injury through the inhibition of TNF- α and iNOS induction in D-galactosamine and LPS-treated rats. *Shock* 2008; **29**: 740-747 [PMID: 18004231]
- Tanaka H, Uchida Y, Kaibori M, Hijikawa T, Ishizaki M, Yamada M, Matsui K, Ozaki T, Tokuhara K, Kamiyama Y, Nishizawa M, Ito S, Okumura T. Na⁺/H⁺ exchanger inhibitor, FR183998, has protective effect in lethal acute liver failure and prevents iNOS induction in rats. *J Hepatol* 2008; **48**: 289-299 [PMID: 18096265 DOI: 10.1016/j.jhep.2007.09.017]
- Uchida Y, Kaibori M, Hijikawa T, Ishizaki M, Ozaki T, Tanaka H, Matsui K, Tokuhara K, Kwon AH, Kamiyama Y, Okumura T. Protective effect of neutrophil elastase inhibitor (FR136706) in lethal acute liver failure induced by D-galactosamine and lipopolysaccharide in rats. *J Surg Res* 2008; **145**: 57-65 [PMID: 17936791 DOI: 10.1016/j.jss.2007.04.001]
- Qi Z, Whitt I, Mehta A, Jin J, Zhao M, Harris RC, Fogo AB, Breyer MD. Serial determination of glomerular filtration rate in conscious mice using FITC-inulin clearance. *Am J Physiol Renal Physiol* 2004; **286**: F590-F596 [PMID: 14600035 DOI: 10.1152/ajprenal.00324.2003]
- Wang E, Sandoval RM, Campos SB, Molitoris BA. Rapid diagnosis and quantification of acute kidney injury using fluorescent ratio-metric determination of glomerular filtration rate in the rat. *Am J Physiol Renal Physiol* 2010; **299**: F1048-F1055 [PMID: 20685826 DOI: 10.1152/ajprenal.00691.2009]
- Soveri I, Berg UB, Björk J, Elinder CG, Grubb A, Mejare I, Sterner G, Bäck SE. Measuring GFR: a systematic review. *Am J Kidney Dis* 2014; **64**: 411-424 [PMID: 24840668 DOI: 10.1053/j.ajkd.2014.04.010]
- Hartleb M, Gutkowski K. Kidneys in chronic liver diseases. *World J Gastroenterol* 2012; **18**: 3035-3049 [PMID: 22791939 DOI: 10.3748/wjg.v18.i24.3035]
- Kim SJ, Kim JK, Lee DU, Kwak JH, Lee SM. Genipin protects lipopolysaccharide-induced apoptotic liver damage in D-galactosamine-sensitized mice. *Eur J Pharmacol* 2010; **635**: 188-193 [PMID: 20303938 DOI: 10.1016/j.ejphar.2010.03.007]
- Wang LK, Wang LW, Li X, Han XQ, Gong ZJ. Ethyl pyruvate prevents inflammatory factors release and decreases intestinal

- permeability in rats with D-galactosamine-induced acute liver failure. *Hepatobiliary Pancreat Dis Int* 2013; **12**: 180-188 [PMID: 23558073 DOI: 10.1016/S1499-3872(13)60029-6]
- 22 **Jambekar AA**, Palma E, Nicolosi L, Rasola A, Petronilli V, Chiara F, Bernardi P, Needleman R, Brusilow WS. A glutamine synthetase inhibitor increases survival and decreases cytokine response in a mouse model of acute liver failure. *Liver Int* 2011; **31**: 1209-1221 [PMID: 21745296 DOI: 10.1111/j.1478-3231.2011.02553.x]
 - 23 **Wright G**, Soper R, Brooks HF, Stadlbauer V, Vairappan B, Davies NA, Andreola F, Hodges S, Moss RF, Davies DC, Jalan R. Role of aquaporin-4 in the development of brain oedema in liver failure. *J Hepatol* 2010; **53**: 91-97 [PMID: 20451280 DOI: 10.1016/j.jhep.2010.02.020]
 - 24 **Zeashan H**, Amresh G, Singh S, Rao CV. Protective effect of *Amaranthus spinosus* against D-galactosamine/lipopolysaccharide-induced hepatic failure. *Pharm Biol* 2010; **48**: 1157-1163 [PMID: 20860438 DOI: 10.3109/13880200903168023]
 - 25 **Ghabril M**, Bonkovsky HL, Kum C, Davern T, Hayashi PH, Kleiner DE, Serrano J, Rochon J, Fontana RJ, Bonacini M. Liver injury from tumor necrosis factor- α antagonists: analysis of thirty-four cases. *Clin Gastroenterol Hepatol* 2013; **11**: 558-564.e3 [PMID: 23333219 DOI: 10.1016/j.cgh.2012.12.025]
 - 26 **Arshad MI**, Piquet-Pellorce C, L'Helgoualc'h A, Rauch M, Patrat-Delon S, Ezan F, Lucas-Clerc C, Nabti S, Lehuen A, Cubero FJ, Girard JP, Trautwein C, Samson M. TRAIL but not FasL and TNF α , regulates IL-33 expression in murine hepatocytes during acute hepatitis. *Hepatology* 2012; **56**: 2353-2362 [PMID: 22961755 DOI: 10.1002/hep.25893]
 - 27 **Lu J**, Jones AD, Harkema JR, Roth RA, Ganey PE. Amiodarone exposure during modest inflammation induces idiosyncrasy-like liver injury in rats: role of tumor necrosis factor- α . *Toxicol Sci* 2012; **125**: 126-133 [PMID: 21984482 DOI: 10.1093/toxsci/kfr266]
 - 28 **Deshpande P**, Rausa K, Turner J, Johnson M, Golestaneh L. Acute kidney injury as a causal factor in mortality associated with hepatorenal syndrome. *Hepatol Int* 2011; **5**: 751-758 [PMID: 21484115 DOI: 10.1007/s12072-011-9269-8]
 - 29 **Brooks HL**, Sorensen AM, Terris J, Schultheis PJ, Lorenz JN, Shull GE, Knepper MA. Profiling of renal tubule Na⁺ transporter abundances in NHE3 and NCC null mice using targeted proteomics. *J Physiol* 2001; **530**: 359-366 [PMID: 11158268 DOI: 10.1111/j.1469-7793.2001.0359k.x]
 - 30 **Takahashi N**, Boysen G, Li F, Li Y, Swenberg JA. Tandem mass spectrometry measurements of creatinine in mouse plasma and urine for determining glomerular filtration rate. *Kidney Int* 2007; **71**: 266-271 [PMID: 17149371 DOI: 10.1038/sj.ki.5002033]
 - 31 **Kasiske BL**, Keane WF. Laboratory Assessment of Renal Disease: Clearance, Urinalysis, and Renal Biopsy. Philadelphia, PA: Saunders, 1996
 - 32 **Poola NR**, Bhuiyan D, Ortiz S, Savant IA, Sidhom M, Taft DR, Kirschenbaum H, Kalis M. A novel HPLC assay for pentamidine: comparative effects of creatinine and inulin on GFR estimation and pentamidine renal excretion in the isolated perfused rat kidney. *J Pharm Pharm Sci* 2002; **5**: 135-145 [PMID: 12207866]
 - 33 **Horio M**, Imai E, Yasuda Y, Hishida A, Matsuo S. Simple sampling strategy for measuring inulin renal clearance. *Clin Exp Nephrol* 2009; **13**: 50-54 [PMID: 18827963 DOI: 10.1007/s10157-008-0084-z]
 - 34 **Ahloulay M**, Déchaux M, Laborde K, Bankir L. Influence of glucagon on GFR and on urea and electrolyte excretion: direct and indirect effects. *Am J Physiol* 1995; **269**: F225-F235 [PMID: 7653596]
 - 35 **Garcia FA**, Pinto SF, Cavalcante AF, Lucetti LT, Menezes SM, Felipe CF, Alves AP, Brito GA, Cerqueira GS, Viana GS. Pentoxifylline decreases glycemia levels and TNF- α , iNOS and COX-2 expressions in diabetic rat pancreas. *Springerplus* 2014; **3**: 283 [PMID: 24991532 DOI: 10.1186/2193-1801-3-283]
 - 36 **Martino RB**, Coelho AM, Kubrusly MS, Leitão R, Sampietre SN, Machado MC, Bacchella T, D'Albuquerque LA. Pentoxifylline improves liver regeneration through down-regulation of TNF- α synthesis and TGF- β 1 gene expression. *World J Gastrointest Surg* 2012; **4**: 146-151 [PMID: 22816029 DOI: 10.4240/wjgs.v4.i6.146]

P- Reviewer: Park J, Voigt M **S- Editor:** Ma YJ
L- Editor: Wang TQ **E- Editor:** Zhang DN





Published by **Baishideng Publishing Group Inc**

8226 Regency Drive, Pleasanton, CA 94588, USA

Telephone: +1-925-223-8242

Fax: +1-925-223-8243

E-mail: bpgoffice@wjgnet.com

Help Desk: <http://www.wjgnet.com/esps/helpdesk.aspx>

<http://www.wjgnet.com>



ISSN 1007-9327

